Am J Cancer Res 2023;13(9):3983-4002
www.ajcr.us /ISSN:2156-6976/ajcr0151662

Original Article

REST-repressed lncRNA LINC01801 induces neuroendocrine differentiation in prostate cancer via transcriptional activation of autophagy

Ching-Hsin Chang[1,2], Ting-Yu Cheng[1], Wayne W Yeh[1], Yun-Li Luo[1], Mel Campbell[3], Tse-Chun Kuo[4], Tsai-Wen Shen[1], Yung-Chih Hong[5], Cheng-Han Tsai[6], Yu-Ching Peng[7], Chin-Chen Pan[7], Muh-Hwa Yang[8,9], Jean-Chen Shih[10], Hsing-Jien Kung[3,11], William J Huang[6], Pei-Ching Chang[1,9], Tzu-Ping Lin[5,6]

[1]Institute of Microbiology and Immunology, National Yang Ming Chiao Tung University, Hsinchu 30010, Taiwan; [2]Department of Urology, Taipei Medical University Hospital, Taipei 11031, Taiwan; [3]Comprehensive Cancer Center, University of California at Davis, Sacramento, CA 95817, USA; [4]Institute of Molecular and Genomic Medicine, National Health Research Institutes, Zhunan, Miaoli 35053, Taiwan; [5]Faculty of Medicine, National Yang Ming Chiao Tung University, Taipei 11221, Taiwan; [6]Department of Urology, Taipei Veterans General Hospital, Taipei 11217, Taiwan; [7]Department of Pathology and Laboratory Medicine, Taipei Veterans General Hospital, Taipei 11217, Taiwan; [8]Institute of Clinical Medicine, National Yang Ming Chiao Tung University, Taipei 11221, Taiwan; [9]Cancer Progression Research Center, National Yang Ming Chiao Tung University, Taipei 11221, Taiwan; [10]Department of Pharmacology and Pharmaceutical Sciences, School of Pharmacy, University of Southern California, Los Angeles, CA 90089, USA; [11]TMU Research Center of Cancer Translational Medicine, Taipei Medical University, Taipei 11031, Taiwan

Received June 9, 2023; Accepted August 3, 2023; Epub September 15, 2023; Published September 30, 2023

Abstract: The association between REST reduction and the development of neuroendocrine prostate cancer (NEPC), a novel drug-resistant and lethal variant of castration-resistant prostate cancer (CRPC), is well established. To better understand the mechanisms underlying this process, we aimed to identify REST-repressed long noncoding RNAs (lncRNAs) that promote neuroendocrine differentiation (NED), thus facilitating targeted therapy-induced resistance. In this study, we used data from REST knockdown RNA sequencing combined with siRNA screening to determine that LINC01801 was upregulated and played a crucial role in NED in prostate cancer (PCa). Using The Cancer Genome Atlas (TCGA) prostate adenocarcinoma database and CRPC samples collected in our laboratory, we demonstrated that LINC01801 expression is upregulated in NEPC. Functional experiments revealed that overexpression of LINC01801 had a slight stimulatory effect on the NED of LNCaP cells, while downregulation of LINC01801 significantly inhibited the induction of NED. Mechanistically, LINC01801 is transcriptionally repressed by REST, and transcriptomic analysis revealed that LINC01801 preferentially affects the autophagy pathway. LINC01801 was found to function as a competing endogenous RNA (ceRNA) to regulate the expression of autophagy-related genes by sponging hsa-miR-6889-3p in prostate cancer cells. In conclusion, our data expand the current knowledge of REST-induced NED and highlight the contribution of the REST-LINC01801-hsa-miR-6889-3p axis to autophagic induction, which may provide promising avenues for therapeutic opportunities.

Keywords: Prostate cancer, neuroendocrine prostate cancer (NEPC), REST, long noncoding RNA (lncRNA)

Introduction

Prostate cancer (PCa) is the second most commonly diagnosed malignancy and the fifth leading cause of cancer-related mortality in men worldwide [1]. Although androgen deprivation therapy (ADT) has been the standard treatment for PCa since 1941 [2], its long-term efficacy is often limited, as the disease may eventually progress to castration-resistant prostate cancer (CRPC) with the reactivation of androgen receptor (AR) signaling [3, 4]. The development of next-generation AR-targeted therapies, such as abiraterone and enzalutamide, has increased the overall survival of patients with CRPC by up to 4.8 months [5-9]. However, some patients

may eventually develop drug resistance, metastasis [10], and progression to neuroendocrine prostate cancer (NEPC) [11].

The emergence of treatment-induced NEPC represents a severe condition because NEPC cells are nonproliferating, terminally differentiated, and express little or no AR, thus rendering them no longer responsive to current ADT and chemotherapy [12]. Furthermore, NEPC cells have been demonstrated to secrete cytokines that promote the growth and chemoresistance of their neighboring prostate adenocarcinoma cells [13, 14]. Therefore, no effective therapy is currently available for NEPC, and patients diagnosed with NEPC have a median overall survival of less than one year [12, 15, 16]. However, the mechanisms underlying the development of NEPC remain obscure.

The molecular features of NEPC have been characterized by reduced or absent expression of AR signature markers and increased expression of NE markers, such as b-tubulin III (TUBIII), synaptophysin (SYP), chromogranin A (CgA), and neuron-specific enolase (NSE) [17, 18]. Genetics and molecular mechanisms associated with the development of androgen independence include loss of the tumor suppressor genes p53 and Rb [19-21], amplification or overexpression of the N-MYC oncogene [22-24], and activation of the neural transcription factor BRN2 [25-27]. However, increasing evidence has suggested that neuroendocrine tumors may develop as a result of lineage plasticity [28], a fundamental developmental process that allows a single genotype to acquire polymorphisms in response to environmental stimuli [29]. This process is particularly notable in the case of NEPC, which has genomic alterations resembling those of CRPC adenocarcinoma [19, 30]. Notably, lineage plasticity has also been associated with the development of drug resistance in response to targeted therapies [31, 32], suggesting the need for increased research into epigenetic regulation of lineage plasticity and its ability to lead to neuroendocrine differentiation (NED) as a potential avenue for the development of novel drug targeting strategies.

In 2014, an understanding of how epigenetic changes in REST-mediated lineage plasticity may drive NED in PCa cells was reported [33-40]. REST, a transcriptional repressor that silences neuronal genes in non-neuronal cells and maintains the pluripotency of neural precursor cells, comprises a DNA-binding domain that recognizes the repressor element-1 (RE-1) site, a 21-nucleotide consensus sequence, and two repressor domains (RD) that recruit Sin3 and CoREST complexes [41]. This capacity to form epigenetic remodeling complexes and suppress target gene transcription has been identified in the regulation of neuroendocrine marker genes [42]. Thus, the decreased expression found during NED in PCa cells indicates a role for epigenetic regulation through REST in the plastic transdifferentiation of NEPC [43, 44].

Long noncoding RNAs (lncRNAs) have recently been defined as a novel type of epigenetic regulator for transcription [45], capable of serving as scaffolds to recruit chromatin-remodeling complexes or transcription factors to specific genomic loci [46-48] or acting as decoys to sequester DNA binding proteins or miRNAs [49]. As such, their regulatory roles in cell development and plasticity have been suggested [50, 51], and dysregulation of lncRNAs has been found to be associated with cancer [52]. Importantly, evidence has demonstrated that lncRNAs may have a role in lineage plasticity-mediated drug resistance [53]. However, research on their role in the regulation of NED in PCa cells is still in its early stages [54, 55]. For example, Crea et al. provided the first evidence for a NEPC-associated lncRNA with the identification of MIAT in 2016 [56]. Furthermore, a recent report suggested that the AR antagonist enzalutamide could promote lncRNA-p21 expression, leading to NED in PCa [57]. In our previous work, we highlighted HOTAIR as a novel REST-regulated lncRNA that participates in PCa cell NED [33]. Therefore, lncRNAs may offer an additional mechanism that enhances NE transdifferentiation of PCa cells.

In this study, a combination of transcriptome analysis and small interfering RNA (siRNA) knockdown screening approaches was used to comprehensively survey lncRNAs. We discovered a previously unrecognized role of long intergenic nonprotein coding RNA 01801 (LINC01801) as a driver of REST-mediated NED. In particular, elevated levels of LINC0-

1801 were detected in CRPC patients with neuroendocrine features, indicating its possible contribution to the development of the NEPC phenotype and its potential use as a biomarker. Additionally, we observed that ectopic expression of LINC01801 results in the induction of autophagy, likely by sponging hsa-miR-6889-3p and upregulating autophagy-related genes. Given that autophagic activation is essential for NED in PCa cells, targeting the LINC01801-hsa-miR-6889-3p axis may impede undesired NED triggered by treatment and thus prevent drug resistance in CRPC.

Materials and methods

Cell culture

LNCaP cells were cultured in RPMI 1640 (Gibco, 31800-014) containing 10% FBS (HyClone, SH30071.03), 1% penicillin/streptomycin and 30 mg/ml L-glutamine (Sigma-Aldrich, G8540). LNCaP-TR cells were cultured as described for LNCaP but supplemented with 5 μg/ml blasticidin S (InvivoGen, ant-bl-1). For the generation of the LINC01801-inducible LNCaP cell line, GeneArt-synthesized LINC01801 cDNA (Thermo Fisher Scientific) was cloned into the pLenti4-CMV/TO vector and introduced into LNCaP-TR cells by lentiviral transduction, followed by selection with 200 μg/ml zeocin (InvivoGen, ant-zn-1). LNCaP-TR-shREST [40] and LNCaP-TR-LINC01801 were maintained as described for LNCaP-TR but supplemented with 50 μg/ml zeocin. All cells were maintained at 37°C in a humidified incubator containing 5% CO_2. For chemo-drug treatment, LNCaP cells were treated with 50 nM enzalutamide (MDV3100; Selleck Chemicals, S1250) for 72 hours.

siRNA transfection

For siRNA screening, LNCaP cells were seeded at 5×10^3 cells/well in 96-well plates and transfected with siRNAs from the Human Lincode siRNA Library (Dharmacon, GU-301000; Lincode® Set of 4 siRNA Library-Human NR lncRNA RefSeq v54, Lot 13101) at a final concentration of 20 nM using Lipofectamine RNAiMAX (Invitrogen, 13778-150) following the manufacturer's protocol. Control siRNA (FITC-conjugated)-A (Santa Cruz, sc-36869) was used as a negative control and to ensure transfection efficiency. For siRNA-mediated knockdown of LINC01801, the siRNA oligonucleotide was purchased from Lincode siRNA Library (Dharmacon, GU-301000); the sequence was 5'-UGAGAAGG-GUACCCAAACA-3'. siRNA was transfected as described above.

High-throughput RNA and small RNA sequencing (RNA-seq and smRNA-seq) and gene ontology (GO) data analysis

Total cellular RNA was extracted from control and knockdown LNCaP cells treated with or without 100 ng/ml IL-6 in phenol red-free RPMI 1640 (Gibco) supplemented with 10% charcoal/dextran-treated FBS (CDT; HyClone, SH-30068.03) and LNCaP-TR-LINC01801 cells treated with or without Dox (1 μg/ml). RNA-seq was performed using the Illumina HiSeq 2000 platform (Illumina, Inc., San Diego, CA, USA). Paired-end reads were then aligned to the human reference genome GRCh37/hg19 using CLC Genomics Workbench (Qiagen, Germantown, MD, USA) and annotated to NONCODE v4.0 with Partek Genomics Suite (Partek, St. Louis, MO, USA). Transcript abundances were calculated using Partek Genomics Suite 7.0, while transcriptome information was obtained from RefSeq Transcripts, NONCODE v4.0, and miRBase v21. For identification of biological functions of differentially expressed mRNAs, a disease and function analysis was conducted using Ingenuity Pathway Analysis (IPA) software.

Real-time reverse transcription and quantitative PCR (real-time RT-qPCR)

Total cellular RNA was isolated by TRIzol reagent (Invitrogen, 15596-018). RNA isolation from paraffin-embedded specimens (FFPE) was carried out using a truXTRAC FFPE RNA kit (Covaris, PN 520161). For the detection of mRNA and lncRNA, cDNA was generated by SuperScript™ III First-Strand Synthesis System Kit (Invitrogen, 18080-085) using Oligo-(dT). Both RNA extraction and cDNA synthesis were performed following the manufacturer's procedure. Real-time qPCR analysis was carried out in 96-well plates with a Bio-Rad CFX96 Real-Time PCR Detection System. All expression levels were normalized against GAPDH. The pairs of qPCR primers were designed by PerlPrimer

(http://perlprimer.sourceforge.net/). The primer sequences are listed in Table S1.

Immunoblotting

Cells were lysed in NP-40 lysis buffer (0.5% NP-40 (Amresco, E109), 1X PBS, and 1X protease inhibitor (Roche, 04693132001)). Protein concentration was measured by Bio-Rad protein assay dye reagent (Bio-Rad, 500-0006) according to the manufacturer's protocol. Protein samples were resolved by SDS-polyacrylamide gel electrophoresis (SDS-PAGE), transferred to 0.45 μm pore size PVDF membranes (GE Healthcare, RPN303F), blocked with 5% BSA in 1X TBST, immunoblotted with primary antibodies against each of the indicated proteins followed by horseradish peroxidase (HRP)-conjugated secondary antibodies, visualized by Pierce ECL Western Blotting Substrate (Thermo Scientific, 34080) and imaged using a Luminescence/Fluorescence Imaging System (Fujifilm, LAS-4000). The primary antibodies used were anti-REST (Millipore, 07-579), anti-TUBIII (Sigma-Aldrich, 2200), anti-CgA (Thermo Fisher Scientific, MA5-13096), anti-SYP (GeneTex, GTX100865), anti-LC3 (Cell Signaling, 2775), anti-AR (Millipore, 06-680), anti-NSE (Cell signaling, 9536), p62 (Cell signaling, 5114) and anti-GAPDH (GTX 100118).

Immunohistochemistry (IHC)

Paraffin-embedded hormone-naïve PCa (HNP) and CRPC tissues were collected at Taipei Veterans General Hospital (TPEVGH). Ethical approval was from the Institutional Review Board (IRB) of TPEVGH. Tissue sections were stained for CgA and visualized as described in our previous report [33]. The expression of CgA in human PCa tissue samples was evaluated using the *H*-score by a board-certified pathologist, Dr. Yu-Ching Peng, in a blind fashion. The *H*-score was derived by multiplying the staining intensity (0-3) by the percentage of epithelial cells with positive staining.

Chromatin immunoprecipitation sequencing (ChIP-Seq) and real-time qPCR

ChIP was performed following the protocol from the Farnham laboratory (http://genomics.ucdavis.edu/farnham). Antibodies were used in ChIP assays as follows: anti-REST (Millipore, 17-641) and nonimmune rabbit serum IgG (Alpha Diagnostic International). ChIP DNA prepared from 2×10^7 LNCaP-TR-shREST cells was subjected to SYBR® Green-based qPCR using a Bio-Rad CFX96 Real-Time PCR System with a primer pair (5'-GCCTTTCTCCCACAATTTCTG-3' and 5'-GTCCCTCTCCATCTCTGTC-3') targeting the LINC01801 promoter of the potential REST binding region identified by ChIP-seq.

Neurite outgrowth assay

LNCaP and LNCaP-TR-LINC01801 cells were seeded on coverslips in 6-well plates at a density of 1×10^5 cells/well. Following treatments as indicated, cells were washed twice with PBS, fixed with 4% paraformaldehyde/PBS for 20 minutes at room temperature, washed twice with PBS, and stained with Cell Membrane Stain (1:2000 dilution in PBS) according to the manufacturer's instructions. Finally, the coverslips were nucleus stained with Hoechst 33342 (Invitrogen, H3569) for 5 minutes at room temperature, mounted in mounting solution (Dako, S3023), visualized/photographed by fluorescence microscopy (Lecia, DMI4000B), and analyzed using MetaMorph (Molecular Devices, Neurite Outgrowth).

miRNA target prediction

DIANA-LncBase v2.0 (http://carolina.imis.athena-innovation.gr) was used to predict the miRNAs that interact with LINC01801 and the mRNAs that can be targeted by hsa-miR-6889-3p.

The Cancer Genome Atlas (TCGA) database

RNA-seq profiles of clinical data from 499 patients with prostate adenocarcinoma and 52 normal prostate tissues were downloaded from TCGA. The expression of LINC01801 was analyzed using two-tailed Student's *t* test.

Results

Identification of lncRNA LINC01801 as a novel neuroendocrine modulator in PCa

Following recent studies indicating that REST may be a prominent regulator of neuroendocrine differentiation (NED) of PCa cells [35-37, 39, 40, 58], particularly when induced by IL-6 treatment [39, 40], and that long noncoding

RNAs (lncRNAs) have emerged as oncogenes or tumor suppressors to regulate lineage plasticity in cancer progression [53], we sought to identify REST-suppressed lncRNAs associated with NED of PCa. First, for identification of potential REST-repressed lncRNAs in PCa cells, transcriptomic data obtained from REST knockdown LNCaP cells (LNCaP-TR-shREST) [36] were reannotated with the NONCODE v4.0 database [59]. According to the repressive nature of REST, more of the 27,661 expressed lncRNAs were found to be upregulated (7,913; 28%) than downregulated (4,774; 17%) after REST knockdown induced by doxycycline (Dox) (**Figure 1A**). Next, we employed siRNA screening utilizing the human Lincode siRNA library, which contained four different siRNAs designed to target each transcript (**Figure 1B**). The NED of PCa cells was monitored through an image-based inspection of the neurite-like morphology of LNCaP cells under IL-6 induction conditions.

An initial screening of 147 long intergenic noncoding RNAs (lincRNAs) present in the human Lincode siRNA library revealed that 14 of them were essential for IL-6-induced NED in LNCaP cells (**Figure 1B**). Further analysis of expression levels under NED induction conditions, including REST knockdown (**Figure 2A**) and IL-6 treatment (**Figure 2B**), identified LINC01801. Consistently, we found higher expression of LINC01801 in DU-145 cells (AR-negative and NE-like cells) [60] than in LNCaP cells (**Figure 2C**). Importantly, we found that treatment with enzalutamide could also induce NED concomitantly with decrease in the level of REST (**Figure 2D**), and increase the expression of LINC01801 (**Figure 2E**) in both LNCaP and C4-2B cells, supporting the notion of REST as a master epigenetic regulator of NED and suggesting that LINC01801 may be involved in REST-induced NED.

We then examined the expression of LINC01801 in clinical samples from the TCGA database and discovered a slight, but not statistically significant, increase in the expression of LINC01801 in prostate adenocarcinoma samples compared to normal prostate tissues (**Figure 2F**, upper panel). In particular, a significantly higher expression of LINC01801 was found in the group that exhibited the highest (top 20%; $TUBIII^{High}$) levels of the neuroendocrine marker b-tubulin III (TUBIII) compared to that of the group that showed the lowest (bottom 20%; $TUBIII^{Low}$) (**Figure 2F**, lower panel), suggesting that LINC01801 expression increases in NEPC rather than in adenocarcinoma. Importantly, we assayed eight human hormone-naïve prostate cancer (HNP) and twenty-six CRPC samples and found an increase in LINC01801 in neuroendocrine marker chromogranin A (CgA)-high samples compared to CgA-low and HNP samples (**Figure 2G**). Together, these data suggest that the expression of LINC01801 is increased in NEPC cells.

LINC01801 as a novel REST-repressive NED driver of PCa cells

To explore the role of LINC01801 in the NED of PCa, we generated an inducible LINC01801-overexpressing LNCaP cell line using LNCaP-TR cells. Subsequent experiments utilizing RT-qPCR, Western blot, and morphological assays showed that LINC01801 induction triggered an increase in the expression of neuroendocrine markers and neurite-like morphological features in LNCaP cells, indicating its link to NED (**Figure 3**). Next, the siRNA approach was used to knock down LINC01801 in LNCaP cells. Importantly, LINC01801 knockdown blocked the REST knockdown-induced NE-like cellular morphology and the expression of REST-suppressed NE markers (**Figure 4A-D**), as well as NED induced by IL-6 treatment (**Figure 4E-H**) of LNCaP cells. Collectively, our data demonstrate that LINC01801 is essential for REST-mediated NED.

Next, we investigated whether LINC01801 is a direct target of REST by searching for REST binding sites (RE-1) in the promoter region (TSS ± 2000) using JASPAR (http://jaspar.genereg.net/). Unexpectedly, no RE-1 site was identified within this region; however, possible REST binding sites were detected on the LINC01801 promoter in multiple cell lines via REST ChIP-seq from the ENCODE database (**Figure 5A**). We then examined our ChIP-seq data for possible REST binding sites in LNCaP cells [33] and revealed multiple potential REST binding regions on the LINC01801 promoter (**Figure 5B**). To verify this, we employed ChIP-qPCR in LNCaP-TR-shREST cells and found that REST was indeed bound to the LINC01801 promoter region, with a significant decrease in recruit-

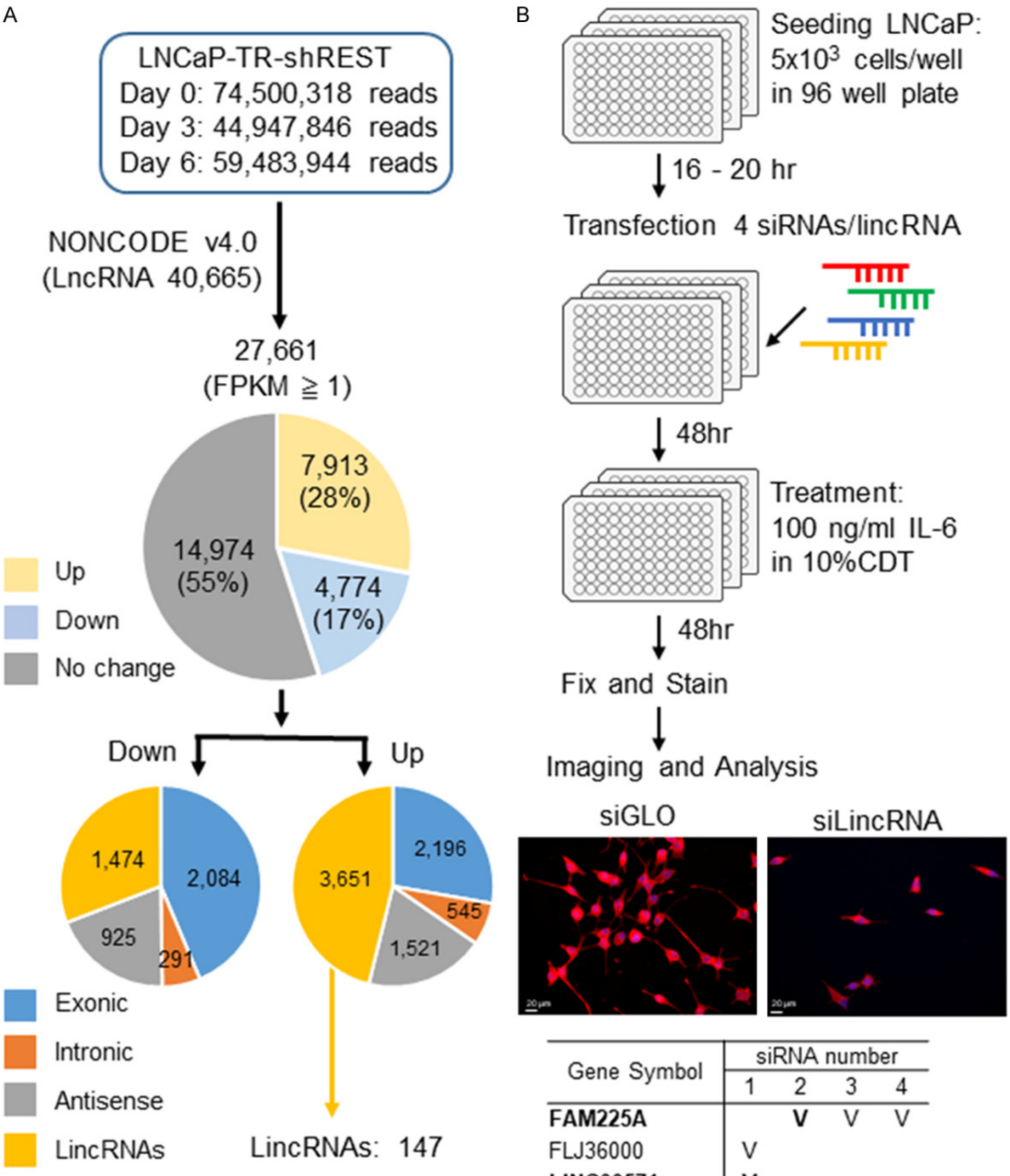

Gene Symbol	siRNA number			
	1	2	3	4
FAM225A		**V**	V	V
FLJ36000	V			
LINC00571	**V**			
LINC00926		**V**		
LINC01000		**V**		
LINC01021	V		**V**	
LINC01801				**V**
LOC100131289				V
LOC100506082				V
LOC100506207				**V**
LOC100506804		**V**		
LOC646736			**V**	
MAFG-AS1			**V**	
NCRUPAR				**V**
SNHG8				**V**
SSSCA1-AS1				**V**
TPT1-AS1				**V**

Figure 1. Identification of LINC01801 as a novel REST-repressed lncRNA required for IL-6-induced NED of LNCaP cells. A. Workflow showing the steps in the identification of REST-targeting long noncoding RNAs (lncRNAs): LNCaP-TR-shREST cells were treated with 1 μg/ml doxycycline (Dox) for 0, 3, and 6 days. Total RNA was extracted and used for RNA sequencing (RNA-seq) to identify lncRNAs with expression levels greater than 1 FPKM in at least one sample. Pie chart showing the number (percentage) of lncRNAs that were up- or downregulated more than 1.5-fold. B. Schematic representation of siRNA-based screening procedure to identify lncRNAs driving NED of LNCaP cells. Representative images show that lncRNA knockdown inhibited IL-6-induced NED neurite outgrowth, with a scale bar of 20 μm. An accompanying table is provided, describing seventeen upregulated lncRNAs whose knockdown reduces IL-6-induced NED of LNCaP cells. Numbers one to four indicate individual siRNA, and lncRNAs that scored in both screens are highlighted in bold.

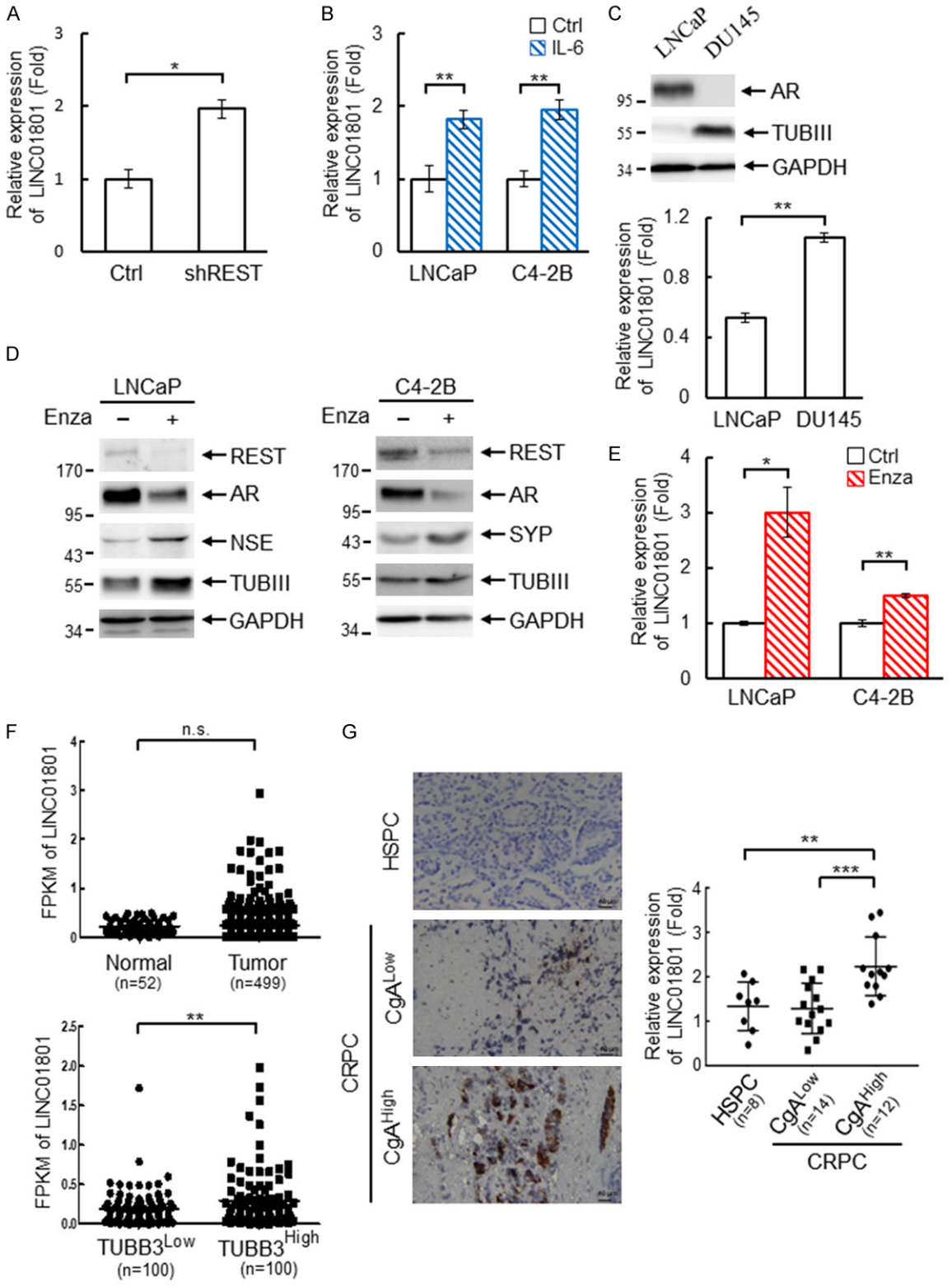

Figure 2. The LINC01801 level is increased in NEPC cells. (A) RT-qPCR analysis to detect LINC01801 expression in LNCaP-TR-shREST cells treated with 1 μg/ml Dox for 72 hours. The cells without treatment were used as the control (Ctrl). (B) RT-qPCR analysis of LINC01801 expression in LNCaP and C4-2B cells after treatment with 100 ng/ml IL-6 in phenol red-free RPMI-1640 with 10% CDT for 72 hours. (C) Immunoblots of AR and TUBIII in LNCaP and DU145. Detecting LINC01801 expression in LNCaP and DU-145 cells by RT-qPCR analysis. (D) Immunoblots of REST, AR and NED markers in LNCaP (left panel) and C4-2B (right panel) cells treated with 50 nM enzalutamide (Enza) for

72 hours. (E) Expression of LINC01801 was measured in LNCaP and C4-2B cells treated as described in (D) by RT-qPCR. The cells without treatment were used as the control (Ctrl). (F) Comparison of LINC01801 levels in tumorous and nontumorous tissues of the prostate dataset from The Cancer Genome Atlas (TCGA) (upper panel) and between samples with high (top 20%) and low (bottom 20%) expression of TUBIII (lower panel). (G) Representative images of IHC staining of CgA show negative staining in hormone-naïve prostate cancer (HNP) and positive staining in CRPC. RT-qPCR analysis of LINC01801 expression in 8 HSPC, 14 CgA low (CgA^{Low}), and 12 CgA high (CgA^{High}) CRPC specimens. For (A-C, E), data are presented as the mean ± SD. The statistical significance was calculated using Student's t test. *P<0.05, **P<0.01, ***P<0.001. n.s. nonsignificant.

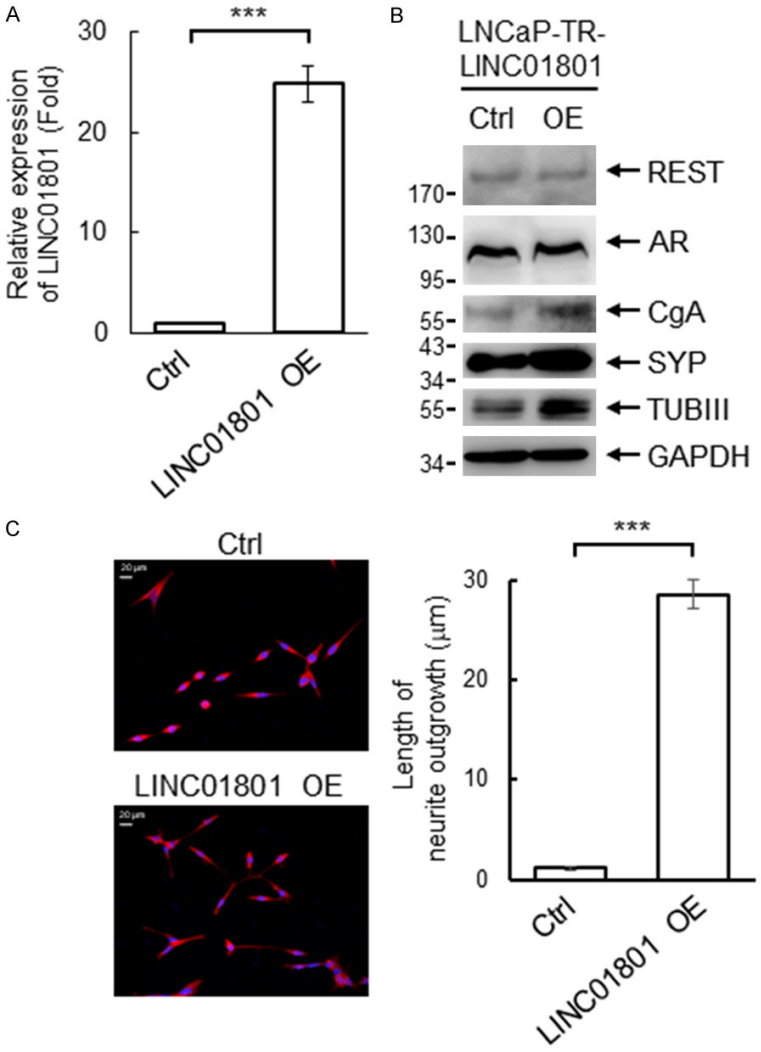

Figure 3. LINC01801 induces NED of LNCaP cells. (A) RT-qPCR analysis to detect LINC01801 expression in LNCaP-TR-LINC01801 cells treated with 0.1 μg/ml Dox for 72 hours. The cells without treatment were used as control (Ctrl). (B) Immunoblots of REST, AR and NED markers in LNCaP-TR-LINC01801 cells treated as described in (A). (C) Representative images (20× magnification) of LNCaP-TR-LINC01801 cells treated as described in (A) and stained by cell membrane stain (red). Scale bar: 20 μm (left panel). Neurite length was quantified by the average from 50 cells (right panel). For (A and C), data are presented as the mean ± SD. The statistical significance was calculated using Student's t test. ***P<0.001.

ment after REST was knocked down (**Figure 5C**). To further validate REST-mediated transcriptional repression of LINC01801, we used LNCaP-TR-REST cells generated in our previous study, which induce overexpression of REST [40]. Dox was administered to cells prior to IL-6 stimulation, and the results demonstrated that REST overexpression attenuated the induction of LINC01801 (**Figure 5D**). Thus, we conclude that LINC01801 is a direct REST-repressed lncRNA that is upregulated in neuroendocrine PCa cells upon downregulation of REST.

LINC01801 modulates the autophagy pathway

For determination of the mechanisms by which LINC01801 regulates NED in PCa, the inducible LINC01801 overexpressing LNCaP cell line was subjected to RNA-seq-based transcriptome profiling. This analysis revealed 8,028 expressed mRNAs with FPKM greater than 1, with 985 (12%) genes being upregulated and 294 (4%) being downregulated. Then, we performed Gene Ontology (GO) data analysis to identify enriched pathways using Ingenuity Pathway Analysis (IPA). The results indicated that genes regulated by LINC01801 overexpression were positively associated with cell viability, autophagy, and gene transcription (**Table 1**).

Next, siRNA was used to knock down LINC01801 in LNCaP cells, which were then

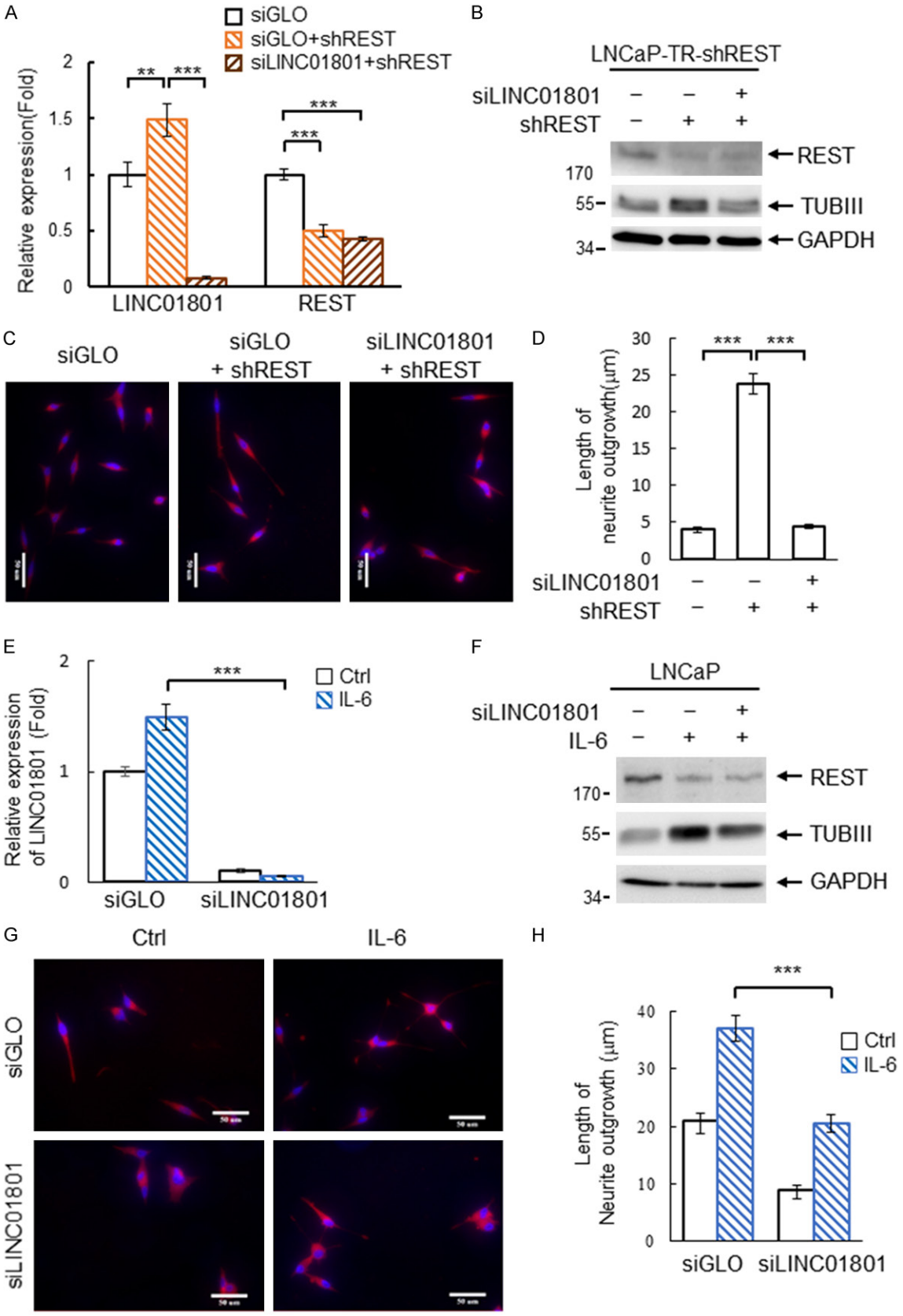
A
siGLO
siGLO+shREST
siLINC01801+shREST
Relative expression(Fold)
LINC01801
REST
B
LNCaP-TR-shREST
siLINC01801
shREST
REST
TUBIII
GAPDH
170
55
34
C
siGLO
siGLO + shREST
siLINC01801 + shREST
D
Length of neurite outgrowth(μm)
siLINC01801
shREST
E
Ctrl
IL-6
Relative expression of LINC01801 (Fold)
siGLO
siLINC01801
F
LNCaP
siLINC01801
IL-6
REST
TUBIII
GAPDH
170
55
34
G
Ctrl
IL-6
siGLO
siLINC01801
H
Length of Neurite outgrowth (μm)
Ctrl
IL-6
siGLO
siLINC01801

Figure 4. LINC01801 is required to maintain the NE characteristics in LNCaP cells. (A) LNCaP-TR-shREST cells were transfected with either a siRNA targeting LINC01801 or a nontargeting control siRNA (siGLO). Twenty-four hours after transfection, cells were treated with 1 μg/ml Dox for 72 hours, and then, the expression of LINC01801 and REST was measured by RT-qPCR. (B) Immunoblots of REST and the NED marker tubulin III (TUBIII) in LNCaP-TR-LINC01801 cells treated as described in (A). (C, D) Representative images (40× magnification) of LNCaP-TR-shREST cells treated as in (A) and stained by cell membrane stain (red) (C); subsequently, neurite length was calculated from the average of 50 cells (D). (E) LNCaP cells were transfected with either siRNA targeting LINC01801 or siGLO for 48 hours and then treated with 100 ng/mL IL-6 in phenol red-free RPMI-1640 with 10% CDT for 48 hours. RT-qPCR was performed to detect LINC01801. (F) Immunoblots of REST and the NED marker tubulin III (TUBIII) in LNCaP cells treated as described in (E). (G, H) Representative images (40× magnification) of LNCaP cells treated as in (E) and stained by cell membrane stain (red) (G); subsequently, neurite length was calculated from the average of 50 cells (H). For (A, D, E, H), data are presented as the mean ± SD. The statistical significance was calculated using Student's t test. ***P*<0.01, ****P*<0.001.

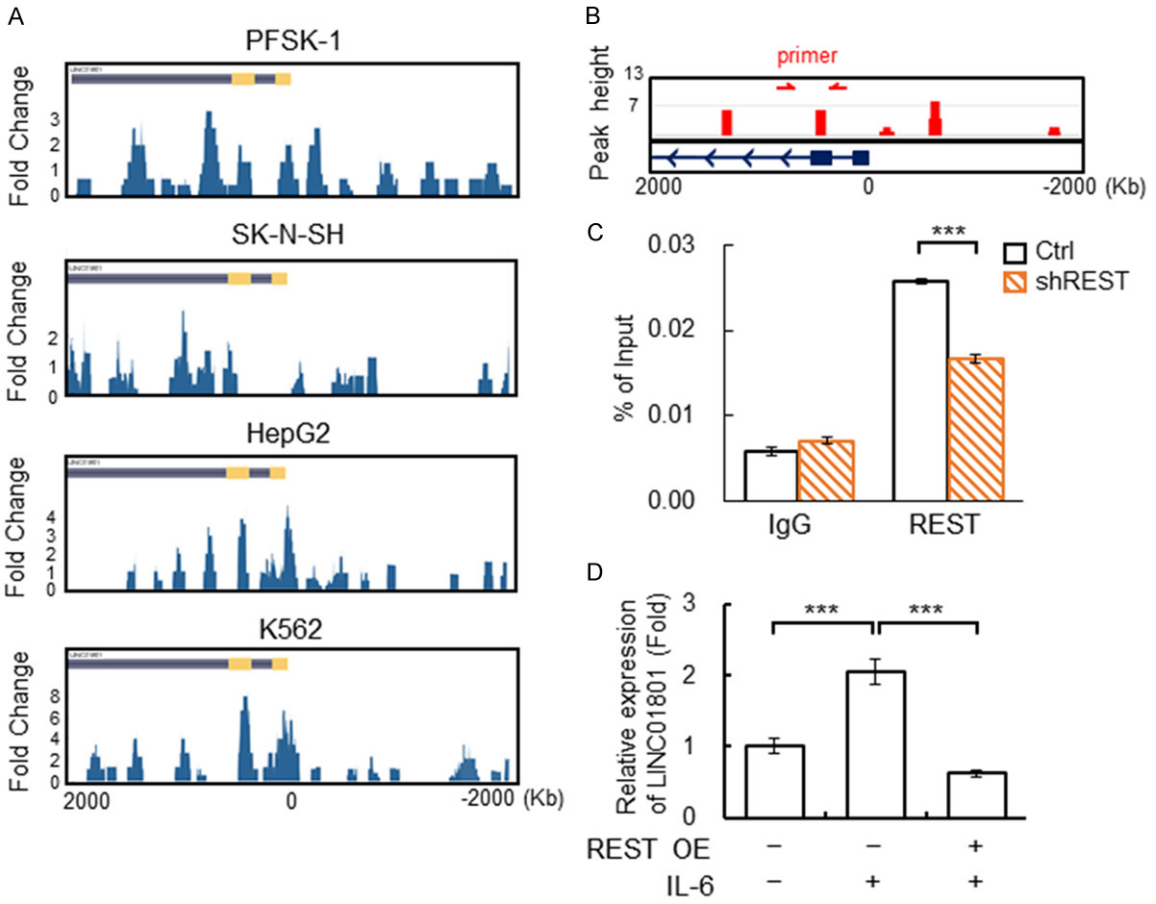

Figure 5. LINC01801 is a direct target of REST. (A) ChIP-seq data of REST binding sites in the LINC01801 promoter region (TSS ± 2000 bp) from the four cell lines PFSK-1, SK-N-SH, HepG2, and K562 were obtained from the ENCODE database. (B) ChIP-seq data of REST binding sites in the LINC01801 promoter region in LNCaP cells. (C) ChIP DNA from LNCaP-TR-shREST cells with or without Dox treatment was precipitated with anti-REST or anti-rabbit IgG and then amplified by qPCR using primers designed for the LINC01801 promoter. (D) RT-qPCR analysis of LINC01801 in LNCaP-TR-REST cells treated as indicated for 72 hours. For (C and D), data are presented as the mean ± SD. The statistical significance was calculated using Student's t test. ****P*<0.001.

treated with IL-6. Subsequently, RNA-seq analysis revealed that after knockdown of LINC01801, 1,167 (11%) genes were upregulated and 2,098 (20%) were downregulated. Furthermore, in the IL-6-treated LINC01801 knockdown LNCaP cells, 297 (3%) genes were upregulated, and 968 (9%) were downregulated. An unbiased functional annotation using IPA revealed that IL-6 treatment had a consistent effect on cells as LINC01801 overexpres-

Table 1. GO categories of LINC01801-regulated genes

Disease & Function	LINC01801		IL-6	
	OE	KD	siGLO	siLINC01801
Cell death and survival				
Cell viability	6.3	-	4.6	5.3
Cell morphology, cellular Function and maintenance				
Autophagy	3.2	-	3.1	-
Autophagy of cells	3.2	-	2.8	-
Gene expression				
Expression of RNA	2.2	-	4.1	-
Transcription	2.2	-	4.4	-

sion, including increased cell viability, autophagy, and gene transcription (**Table 1**). Notably, knockdown of LINC01801 selectively abolished the autophagy and gene expression pathways induced by IL-6 but had less of an effect on modulation of the canonical cell viability pathway (**Table 1**). These results support the hypothesis that autophagy is essential for IL-6-induced NED in PCa [40, 61], further suggesting that LINC01801 may be a downstream target of REST that regulates autophagy-related gene expression and activates autophagy in NED processes.

LINC01801 activates autophagy through transcriptional upregulation of autophagy-related genes

To confirm whether autophagy is activated by LINC01801, we examined its activation in LNCaP cells overexpressing LINC01801. The results showed an increase in autophagic cells (**Figure 6A**) and LC3-II levels (**Figure 6B**). These findings are consistent with previous reports, including our own [36, 40, 61], showing that autophagy is activated and required for NED.

Given that the IPA analysis showed an association between LINC01801 and gene expression, the levels of 19 genes defined in the autophagy pathway were measured by RT-qPCR. The results showed that LINC01801 overexpression increased the expression of ATM, HIF1A, PTEN, TBK1, VPS13A, and XPO1 (**Figure 6C**). Subsequently, a clinical survey based on the TCGA database was conducted, which revealed that the expression levels of the aforementioned genes were significantly higher among those with the highest (top 20%; LINC01801^{High}) levels of LINC01801 compared to those with the lowest (bottom 20%; LINC01801^{Low}) levels (**Figure 6D**). Furthermore, the expression levels of autophagy-related genes in the TUBIII^{High} group were compared with those in the TUBIII^{Low} group, and similarly, the expression levels of HIF1A, PTEN, VPS13A and XPO1 were higher in the TUBIII^{High} group (**Figure 6E**). Collectively, these findings further support the notion that LINC01801 is involved in NED by regulating the expression of autophagy-related genes and activating autophagy.

LINC01801 activates the autophagy pathway by sponging miR-6889-3p and upregulating autophagy-related genes

Given that lncRNAs can modulate gene transcription by sponging miRNAs, which results in co-up- and co-downregulation of their target genes, and the fact that most of the LINC01801-regulated mRNAs were co-up- and co-downregulated with LINC01801, we hypothesized that LINC01801 may function as a ceRNA to modulate gene expression. To study this, we first determined the subcellular distribution of LINC01801 using an RNA scope assay. Our results showed that, consistent with the cytoplasmic localization of ceRNAs, LINC01801 was predominantly found in the cytoplasmic compartment, albeit to a lesser extent in the nuclear compartment (**Figure 7A**). To identify miRNAs potentially sponged by LINC01801, we performed smRNA-seq to profile miRNA expression in the IL-6-treated LNCaP cells with/without knockdown of LINC01801. Among the 725 expressed miRNAs, 47 (6%) were upregulated and 179 (25%) were downregulated after IL-6 treatment. Notably, knockdown of LINC01801 under IL-6 treatment conditions significantly increased the number of upregulated miRNAs (157 miR-

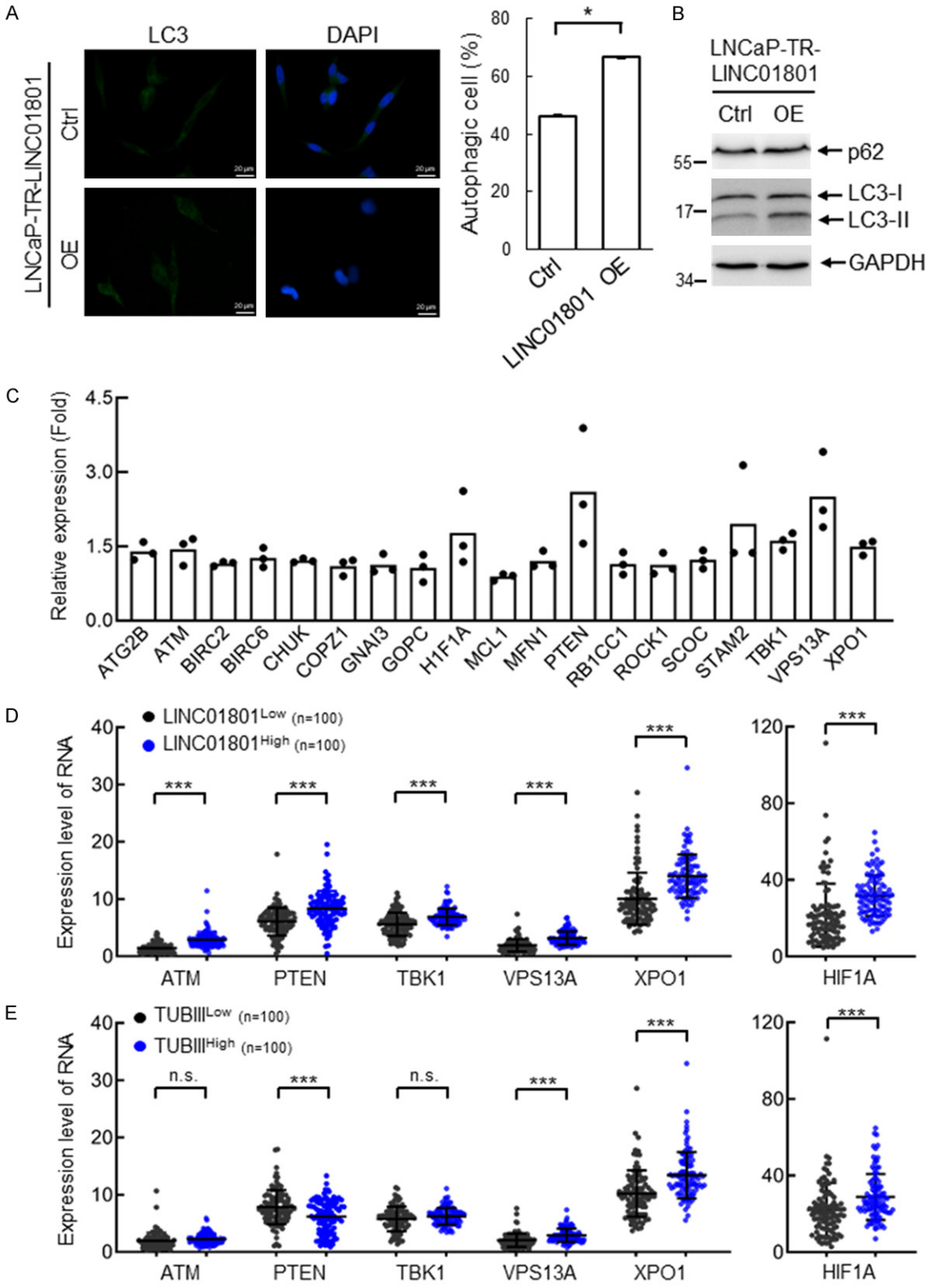

Figure 6. Overexpression of LINC01801 activates the autophagy pathway through upregulation of autophagy-related genes. (A) Representative images (64× magnification) of LNCaP-TR-LINC01801 cells treated with or without 0.1 μg/ml Dox for 72 hours and stained with anti-LC3 antibody (Green) and Hoechst 33342 (blue). The cells without treatment were used as a control (Ctrl). Scale bar: 20 μm (left panel). Quantitative analysis of the average from 5 microscopic fields was used to assess autophagic cell number (right panel). (B) Immunoblots of p62 and LC3

in LNCaP-TR-LINC01801 cells treated as described in (A). (C) RT-qPCR was used to detect the expression of 19 autophagy-related genes in LNCaP-TR- LINC01801 cells treated as described in (A). (D, E) The levels of the six LINC01801 upregulated genes in LINC01801 (D) and TUBIII (E) high (top 20%) and low (bottom 20%) prostate adenocarcinoma samples from the TCGA database. The statistical significance was calculated using Student's t test. **P*<0.05, ****P*<0.001. n.s. nonsignificant.

NAs; 22%) compared to IL-6 treatment alone (47 miRNAs; 6%), suggesting a role for LINC01801 as a ceRNA. To further investigate this hypothesis, we used the DIANA-LncBase v2.0 database to predict potential miRNAs that may be targeted by LINC01801. We found that of the 179 miRNAs downregulated by IL-6 treatment, 9 were predicted to be potential targets for LINC01801 (**Figure 7B**). Additionally, for the 157 miRNAs upregulated after knockdown of LINC01801 under IL-6 treatment conditions, 10 miRNAs were predicted as potential targets of LINC01801 (**Figure 7B**). Notably, the miRNAs hsa-miR-3620-3p, hsa-miR-6515-3p and hsa-miR-6889-3p were common targets of these two groups (**Figure 7B**, bold).

To investigate whether these miRNAs were targeted by LINC01801, we performed RT-qPCR on LINC01801-overexpressing LNCaP cells and identified hsa-miR-6889-3p as a potential target of LINC01801 (**Figure 7C**). Supporting the notion that ceRNA possesses multiple binding sites for its targeted miRNA, LINC01801 contains 5 potential binding sites for hsa-miR-6889-3p (**Figure 7D**). To determine whether hsa-miR-6889-3p participates in LINC01801-induced autophagy activation, we transfected a hsa-miR-6889-3p mimic into LNCaP-TR-LINC01801 cells. The results demonstrated that the hsa-miR-6889-3p mimic inhibited the autophagy induced by overexpression of LINC01801 (**Figure 7E**). Additionally, the expression of autophagy-related genes was analyzed, and the hsa-miR-6889-3p mimic was found to inhibit the expression of ATM, HIF1A, PTEN, VPS13A, and XPO1, and the overexpression of LINC01801 partially reversed the suppressive effect of hsa-miR-6889-3p on HIF1A, PTEN, and VPS13A (**Figure 7F**). Unfortunately, the potential hsa-miR-6889-3p target site on the transcript of most autophagy genes, except PTEN, could not be detected using various bioinformatic tools, such as TargetScan, miRTar base, and TarBase. This finding suggests that hsa-miR-6889-3p likely represses autophagy-related gene expression through an indirect mechanism, which warrants further investigation. In conclusion, our findings suggest that the LINC01801-hsa-miR-6889-3p axis is responsible for REST-mediated control of NED and autophagic activation.

Discussion

New generations of anti-AR therapies have been developed to treat metastatic CRPC. However, these new therapies may induce adverse effects, particularly increasing the prevalence of NEPC. Given the poor prognosis and lack of effective treatments, the average survival rate after NEPC diagnosis is less than a year [62]. Therefore, more research is necessary to elucidate the molecular mechanisms behind NEPC for improved prevention and control of this type of CRPC.

The progression of PCa to CRPC has been demonstrated to occur via diverse mechanisms, particularly gene mutations and amplifications [21, 24]. Notably, lineage plasticity has the potential to minimize the AR dependence of CRPC, thereby facilitating the acquisition of an NE phenotype [28]. Furthermore, epigenetic regulatory control over transcriptional accessibility has been identified as a fundamental factor in mediating the plasticity of NEPC [43, 44]. Due to its potentially reversible nature, in contrast to irreversible genetic events with few effective targeted therapies, it is of particular interest to study epigenetics in the progression of CRPC to NEPC. For example, EZH2, a histone H3 lysine-27 tri-methyl (H3K27me3) methyltransferase, epigenetically mediates NED. Inhibition of EZH2 suppresses NED and sensitizes AR-targeted therapy [22, 57]. However, to date, no epigenetic therapeutic intervention has been clinically approved.

Downregulation of REST, a transcriptional repressor known to regulate neuronal differentiation [63, 64] and tumor growth [65, 66], was observed in up to 50% of clinical NEPC specimens [67]. In 2014, evidence emerged for the first time indicating that REST serves as a critical epigenetic repressor that governs the NED driver gene in PCa [37]. Consistent with this

A

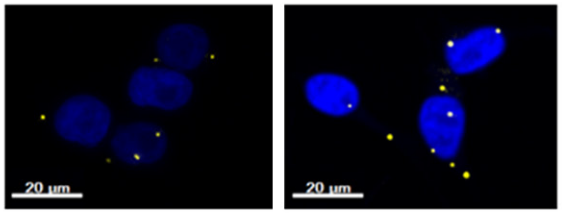

B

microRNA	IL-6 (Down)	siLINC01801 (Up)	lncBase Target predict (#)
hsa-miR-3182	+		5
hsa-miR-3620-3p	+	+	**3**
hsa-miR-3942-3p	+		5
hsa-miR-423-5p	+		2
hsa-miR-4482-3p	+		1
hsa-miR-4531	+		3
hsa-miR-6515-3p	+	+	**2**
hsa-miR-6889-3p	+	+	**5**
hsa-miR-942-5p	+		1
hsa-miR-191-3p		+	1
hsa-miR-4690-3p		+	1
hsa-miR-6516-5p		+	3
hsa-miR-6737-3p		+	4
hsa-miR-6742-3p		+	3
hsa-miR-6852-5p		+	4
hsa-miR-6894-3p		+	5

C

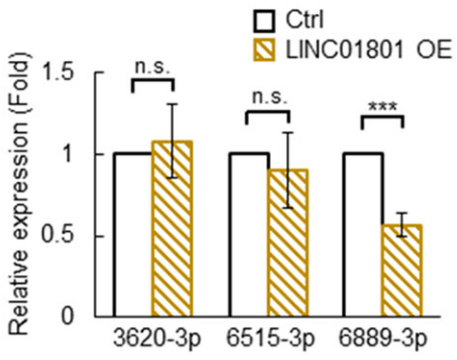

D

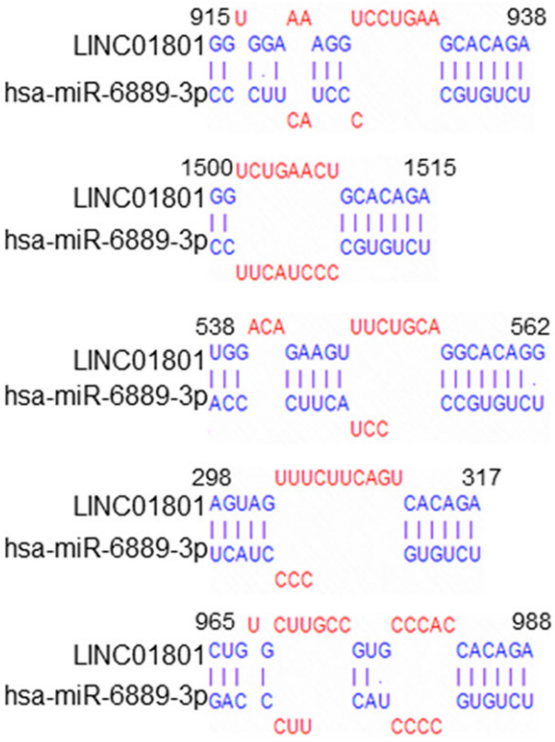

E

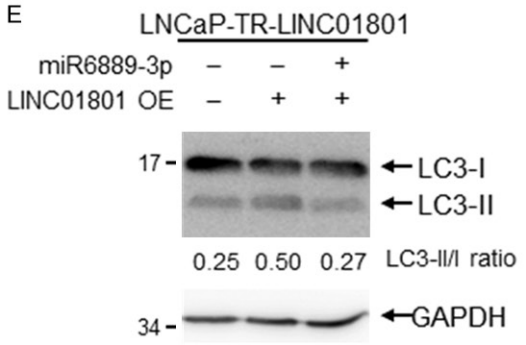

F

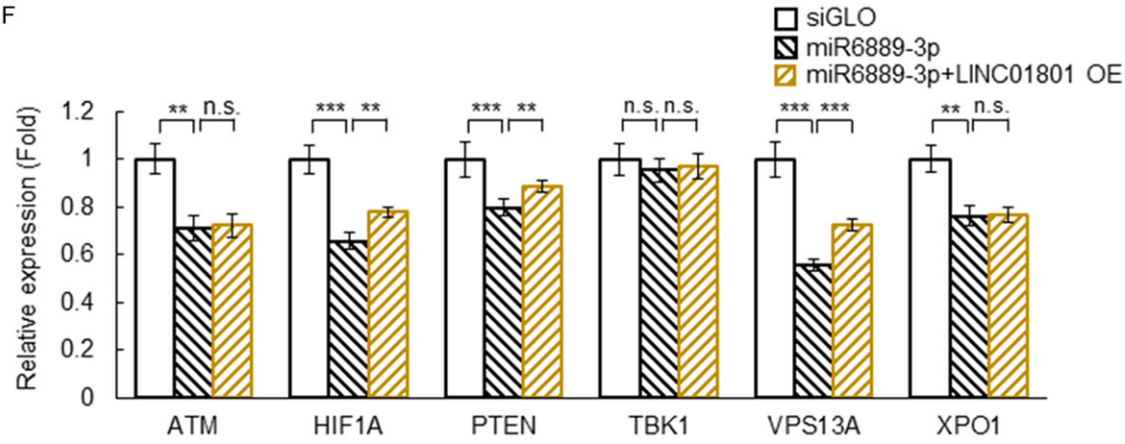

Figure 7. hsa-miR-6889-3p as a potential target of LINC01801. (A) Representative RNAscope images (40× magnification) of LNCaP cells treated with 100 ng/ml IL-6 in phenol red-free RPMI-1640 with 10% CDT compared with the untreated cells (Ctrl). Scale bar: 20 μm. (B) Prediction of LINC01801 targeted miRNAs, which are downregulated with IL-6 treatment and upregulated after knockdown of LINC01801 using DIANA-LncBase v2.0. (C) The expression levels of hsa-miR-3620-3p, hsa-miR-6515-3p, and hsa-miR-6889-3p in LNCaP-TR-LINC01801 cells treated with or without 0.1 μg/ml Dox for 72 hours. (D) The structure of the predicted hsa-miR-6889-3p binding site on LINC01801. (E) Immunoblots of LC3 in Dox-treated LNCaP-TR-LINC01801 cells transiently transfected with hsa-miR-6889-3p mimic or siGLO. Cells without any treatment were used as the control (Ctrl). (F) RT-qPCR was used to detect the expression of the six LINC01801 upregulated genes (**Figure 6**) in LNCaP-TR-LINC01801 cells treated as described in (E). The statistical significance was calculated using Student's t test. $^{**}P<0.01$, $^{***}P<0.001$. n.s. nonsignificant.

finding, our previous reports have elucidated the role of REST in the regulation of autophagy-related genes, which are required for NED in response to various stimuli [36, 40, 68]. Interestingly, our recent findings further demonstrated that the lncRNA HOTAIR, which is repressed by REST, could potentially serve as an underlying mechanism of NED mediated by REST, suggesting the potential of lncRNA to serve as an underlying mechanism of NED mediated by REST. Furthermore, due to the high tissue specificity of lncRNAs [69], the lncRNA prostate cancer gene 3 (PCA3) has been approved by the Food and Drug Administration (FDA) and is now being used in the clinical setting as a routine biomarker for the diagnosis of PCa [70, 71]. Additionally, lncRNAs may epigenetically regulate transcription by either acting as scaffolds for the recruitment of transcription regulators to certain genomic loci or functioning as competing endogenous RNAs (ceRNAs) to sponge miRNAs [46-49]. Taken together, these findings indicate that lncRNAs may play an important role in initiating and facilitating the progression of NEPC and thus present an opportunity for novel therapies [54, 56, 57].

To identify potential REST-repressed lncRNAs involved in the NED of PCa, we used an inducible REST knockdown LNCaP cell model. Following a comprehensive siRNA knockdown screening, we identified a novel REST-targeted NED-related lncRNA, LINC01801 (Gene ID: 400685; location (hg38): chr19:34788534-34832869). This lncRNA is categorized as a subtype of lncRNA originating from intergenic regions, known as long intergenic noncoding RNA (lincRNA). Although limited information is available, a 2012 study observed deletions of the genomic locus that includes LINC01801 in relation to 19q13.11 deletion syndrome [72], an autosomal dominant neurodevelopmental disorder [73]. This finding suggests that LINC01801 may be involved in mediating lineage plasticity and neuronal differentiation. To further investigate, we conducted immunohistochemical staining (IHC) of CgA in 8 HNP and 26 CRPC tissues. We observed an NE phenomenon in 12 CRPC samples and discovered that LINC01801 expression levels increased greatly in CRPC samples with NE characteristics compared to HNP and CRPC without NE characteristics (**Figure 2G**).

To gain insight into the function of this novel lncRNA, we performed transcriptome analysis in LNCaP cells using overexpression and knockdown approaches. Bioinformatic analysis using IPA revealed that cell viability, autophagy and RNA transcription pathways were significantly enriched in genes regulated by LINC01801 overexpression but not in those regulated by LINC01801 knockdown, as evidenced by z-score hits (≥|2.0|) (**Table 1**). More importantly, IL-6 treatment was found to significantly modulate gene expression in pathways related to cell viability, autophagy, and RNA transcription, while knockdown of LINC01801 via siRNA abolished the autophagy and RNA transcription pathways enriched by IL-6 treatment (**Table 1**). Our findings confirm that IL-6 treatment induces PCa NED through activation of autophagy [40, 61] and suggest that LINC01801 plays a role in this process through transcriptional regulation of autophagy-related genes. Real-time RT-qPCR analysis further supports this concept, as an increase in ATM, HIF1A, PTEN, TBK1, VPS13A, and XPO1 mRNA levels was found after LINC01801 overexpression.

Furthermore, we observed that in the RNA-seq data, the number of genes upregulated by LINC01801 overexpression (985, 12%) was higher than that downregulated (294, 4%), while the number of genes downregulated (2,098, 20%) after siLINC01801 knockdown

was higher than that of genes upregulated (1,167, 11%). Similarly, after IL-6 treatment, the downregulated genes (968, 9%) were more pronounced than the upregulated genes (297, 3%) following LINC01801 knockdown. Given that lncRNAs play a key role in mediating transcription by sponging miRNAs and the observation of co-up- and co-downregulation of LINC01801 with genes regulating autophagy, LINC01801 may possess ceRNA activity and affect the NED process, at least in part, by sponging miRNAs. To identify miRNAs that can be sequestered by LINC01801 and are also related to NE differentiation, we performed smRNA-seq of IL-6-treated LNCaP cells with or without LINC01801 knockdown. The results showed that under IL-6 treatment, 179 miRNAs (25%) were downregulated and 47 (6%) were upregulated, while under LINC01801 knockdown, 157 miRNAs (22%) were upregulated. This finding further supported the notion that LINC01801 has the ability to sponge miRNAs and function as a ceRNA. To investigate potential miRNAs that are targeted by lncRNA LINC01801, we used DIANA-LncBase v2.0 to predict miRNA-interacting regions on LINC01801. After examining the miRNAs that were downregulated in IL-6 treatment and upregulated after LINC01801 knockdown, we identified three candidates (**Figure 7B**). In particular, hsa-miR-6889-3p, which contained five potential binding sites on LINC01801, was found to decrease its expression levels following overexpression of LINC01801 (**Figure 7C**). The ratio between the number of miRNA-binding sites in lncRNAs and the levels of miRNA molecules may play an essential role in ceRNA regulation [74]. In this regard, hsa-miR-6889-3p, which has five potential binding sites on LINC01801 and is expressed at a relatively low level (RPM ~1), with a ranking of 644th out of 725 expressed miRNAs (RPM >1) in LNCaP cells, may be a possible target of regulation by LINC01801.

Surprisingly, we were unable to identify target sites for hsa-miR-6889-3p in most upregulated autophagy-related genes after LINC01801 overexpression. However, we verified that hsa-miR-6889-3p regulation of most LINC01801 upregulated autophagy-related genes via an overexpression assay, while overexpression of LINC01801 partially reversed the expression of some of these genes (**Figure 7F**). Among them, HIF1A is transcriptionally activated and stabilized by STAT3 under hypoxic conditions, resulting in autophagic induction [75]. VPS13A is a phospholipid transporter implicated in the packaging of organelles into autophagosomes and has recently been found to be an autophagy-regulated gene [76]. Taken together, our data suggest that the LINC01801-hsa-miR-6889-3p axis may modulate autophagy-related genes through an indirect mechanism that warrants further exploration.

In conclusion, we have identified LINC01801 as a novel REST-targeting lncRNA, and LINC01801-mediated sponging of hsa-miR-6889-3p can restore the expression of autophagy-related genes, activate autophagy and, consequently, induce NED, indicating that LINC01801 could serve as a prognostic biomarker for NEPC and that inhibition of autophagy could be a potential therapeutic approach for treating this highly drug-resistant subtype of CRPC.

Acknowledgements

The authors acknowledge the “technical services” provided by the Genomics Center for Clinical and Biotechnological Applications of the Cancer Progression Research Center (National Yang Ming Chiao Tung University). The National Core Facility for Biopharmaceuticals (NCFB), Ministry of Science and Technology. The work was supported by grants to T.P.L. (MOST 106-2314-B-075-053-MY3 and 109-2314-B-075-072-MY3; NSTC 112-2314-B-A49-055-MY3; NHRI NHRI-109BCC0-MF-202014-03; Taipei Veterans General Hospital, V109C-111, V110C-104, V111C-081, V112C-077; and Yen Ching Ling Medical Foundation, CI-106-17 and CI-110-21) and grants to P.C.C. (MOST 108-2320-B-010-029-MY3 and 111-2320-B-A49-030-MY3; NHRI NHRI-EX111~113-11125BI). This work was financially supported by grants from the Ministry of Education, Higher Education SPROUT Project for Cancer Progression Research Center (111W31101) and Cancer and Immunology Research Center (112W31101).

Disclosure of conflict of interest

None.

Address correspondence to: Pei-Ching Chang, Institute of Microbiology and Immunology, National Yang Ming Chiao Tung University, Hsinchu 30010,

Taiwan. Tel: +886-2-2826-7111; E-mail: pcchang@nycu.edu.tw; Tzu-Ping Lin, Department of Urology, Taipei Veterans General Hospital, Taipei 11217, Taiwan. Tel: +886-2-2875-7519; E-mail: tplin@vghtpe.gov.tw

References

[1] Bray F, Ferlay J, Soerjomataram I, Siegel RL, Torre LA and Jemal A. Global cancer statistics 2018: GLOBOCAN estimates of incidence and mortality worldwide for 36 cancers in 185 countries. CA Cancer J Clin 2018; 68: 394-424.

[2] Huggins C. Effect of orchiectomy and irradiation on cancer of the prostate. Ann Surg 1942; 115: 1192-1200.

[3] Karantanos T, Corn PG and Thompson TC. Prostate cancer progression after androgen deprivation therapy: mechanisms of castrate resistance and novel therapeutic approaches. Oncogene 2013; 32: 5501-5511.

[4] Watson PA, Arora VK and Sawyers CL. Emerging mechanisms of resistance to androgen receptor inhibitors in prostate cancer. Nat Rev Cancer 2015; 15: 701-711.

[5] Bianchini D, Lorente D, Rodriguez-Vida A, Omlin A, Pezaro C, Ferraldeschi R, Zivi A, Attard G, Chowdhury S and de Bono JS. Antitumour activity of enzalutamide (MDV3100) in patients with metastatic castration-resistant prostate cancer (CRPC) pre-treated with docetaxel and abiraterone. Eur J Cancer 2014; 50: 78-84.

[6] Loriot Y, Bianchini D, Ileana E, Sandhu S, Patrikidou A, Pezaro C, Albiges L, Attard G, Fizazi K, De Bono JS and Massard C. Antitumour activity of abiraterone acetate against metastatic castration-resistant prostate cancer progressing after docetaxel and enzalutamide (MDV3100). Ann Oncol 2013; 24: 1807-1812.

[7] Scher HI, Beer TM, Higano CS, Anand A, Taplin ME, Efstathiou E, Rathkopf D, Shelkey J, Yu EY, Alumkal J, Hung D, Hirmand M, Seely L, Morris MJ, Danila DC, Humm J, Larson S, Fleisher M and Sawyers CL; Prostate Cancer Foundation/Department of Defense Prostate Cancer Clinical Trials Consortium. Antitumour activity of MDV3100 in castration-resistant prostate cancer: a phase 1-2 study. Lancet 2010; 375: 1437-1446.

[8] de Bono JS, Logothetis CJ, Molina A, Fizazi K, North S, Chu L, Chi KN, Jones RJ, Goodman OB Jr, Saad F, Staffurth JN, Mainwaring P, Harland S, Flaig TW, Hutson TE, Cheng T, Patterson H, Hainsworth JD, Ryan CJ, Sternberg CN, Ellard SL, Flechon A, Saleh M, Scholz M, Efstathiou E, Zivi A, Bianchini D, Loriot Y, Chieffo N, Kheoh T, Haqq CM and Scher HI; COU-AA-301 Investigators. Abiraterone and increased survival in metastatic prostate cancer. N Engl J Med 2011; 364: 1995-2005.

[9] Scher HI, Fizazi K, Saad F, Taplin ME, Sternberg CN, Miller K, de Wit R, Mulders P, Chi KN, Shore ND, Armstrong AJ, Flaig TW, Flechon A, Mainwaring P, Fleming M, Hainsworth JD, Hirmand M, Selby B, Seely L and de Bono JS; AFFIRM Investigators. Increased survival with enzalutamide in prostate cancer after chemotherapy. N Engl J Med 2012; 367: 1187-1197.

[10] Qin J, Lee HJ, Wu SP, Lin SC, Lanz RB, Creighton CJ, DeMayo FJ, Tsai SY and Tsai MJ. Androgen deprivation-induced NCoA2 promotes metastatic and castration-resistant prostate cancer. J Clin Invest 2014; 124: 5013-5026.

[11] Puca L, Vlachostergios PJ and Beltran H. Neuroendocrine differentiation in prostate cancer: emerging biology, models, and therapies. Cold Spring Harb Perspect Med 2019; 9: a030593.

[12] Aggarwal R, Huang J, Alumkal JJ, Zhang L, Feng FY, Thomas GV, Weinstein AS, Friedl V, Zhang C, Witte ON, Lloyd P, Gleave M, Evans CP, Youngren J, Beer TM, Rettig M, Wong CK, True L, Foye A, Playdle D, Ryan CJ, Lara P, Chi KN, Uzunangelov V, Sokolov A, Newton Y, Beltran H, Demichelis F, Rubin MA, Stuart JM and Small EJ. Clinical and genomic characterization of treatment-emergent small-cell neuroendocrine prostate cancer: a multi-institutional prospective study. J Clin Oncol 2018; 36: 2492-2503.

[13] Hashimoto K, Kyoda Y, Tanaka T, Maeda T, Kobayashi K, Uchida K, Kitamura H, Hirata K, Tsukamoto T and Masumori N. The potential of neurotensin secreted from neuroendocrine tumor cells to promote gelsolin-mediated invasiveness of prostate adenocarcinoma cells. Lab Invest 2015; 95: 283-295.

[14] Cui Y, Sun Y, Hu S, Luo J, Li L, Li X, Yeh S, Jin J and Chang C. Neuroendocrine prostate cancer (NEPCa) increased the neighboring PCa chemoresistance via altering the PTHrP/p38/Hsp27/androgen receptor (AR)/p21 signals. Oncogene 2016; 35: 6065-6076.

[15] Abida W, Cyrta J, Heller G, Prandi D, Armenia J, Coleman I, Cieslik M, Benelli M, Robinson D, Van Allen EM, Sboner A, Fedrizzi T, Mosquera JM, Robinson BD, De Sarkar N, Kunju LP, Tomlins S, Wu YM, Nava Rodrigues D, Loda M, Gopalan A, Reuter VE, Pritchard CC, Mateo J, Bianchini D, Miranda S, Carreira S, Rescigno P, Filipenko J, Vinson J, Montgomery RB, Beltran H, Heath EI, Scher HI, Kantoff PW, Taplin ME, Schultz N, deBono JS, Demichelis F, Nelson PS, Rubin MA, Chinnaiyan AM and Sawyers CL. Genomic correlates of clinical outcome in advanced prostate cancer. Proc Natl Acad Sci U S A 2019; 116: 11428-11436.

[16] Rickman DS, Beltran H, Demichelis F and Rubin MA. Biology and evolution of poorly differentiated neuroendocrine tumors. Nat Med 2017; 23: 1-10.
[17] Frigo DE and McDonnell DP. Differential effects of prostate cancer therapeutics on neuroendocrine transdifferentiation. Mol Cancer Ther 2008; 7: 659-669.
[18] Wang Y, Wang Y, Ci X, Choi SYC, Crea F, Lin D and Wang Y. Molecular events in neuroendocrine prostate cancer development. Nat Rev Urol 2021; 18: 581-596.
[19] Ku SY, Rosario S, Wang Y, Mu P, Seshadri M, Goodrich ZW, Goodrich MM, Labbe DP, Gomez EC, Wang J, Long HW, Xu B, Brown M, Loda M, Sawyers CL, Ellis L and Goodrich DW. Rb1 and Trp53 cooperate to suppress prostate cancer lineage plasticity, metastasis, and antiandrogen resistance. Science 2017; 355: 78-83.
[20] Tan HL, Sood A, Rahimi HA, Wang W, Gupta N, Hicks J, Mosier S, Gocke CD, Epstein JI, Netto GJ, Liu W, Isaacs WB, De Marzo AM and Lotan TL. Rb loss is characteristic of prostatic small cell neuroendocrine carcinoma. Clin Cancer Res 2014; 20: 890-903.
[21] Stone L. Prostate cancer: hand in hand - Rb1 and Trp53 cooperate to suppress resistance. Nat Rev Urol 2017; 14: 131.
[22] Dardenne E, Beltran H, Benelli M, Gayvert K, Berger A, Puca L, Cyrta J, Sboner A, Noorzad Z, MacDonald T, Cheung C, Yuen KS, Gao D, Chen Y, Eilers M, Mosquera JM, Robinson BD, Elemento O, Rubin MA, Demichelis F and Rickman DS. N-Myc induces an EZH2-mediated transcriptional program driving neuroendocrine prostate cancer. Cancer Cell 2016; 30: 563-577.
[23] Lee JK, Phillips JW, Smith BA, Park JW, Stoyanova T, McCaffrey EF, Baertsch R, Sokolov A, Meyerowitz JG, Mathis C, Cheng D, Stuart JM, Shokat KM, Gustafson WC, Huang J and Witte ON. N-Myc drives neuroendocrine prostate cancer initiated from human prostate epithelial cells. Cancer Cell 2016; 29: 536-547.
[24] Sidaway P. Prostate cancer: N-Myc expression drives neuroendocrine disease. Nat Rev Urol 2016; 13: 695.
[25] Bhagirath D, Yang TL, Tabatabai ZL, Majid S, Dahiya R, Tanaka Y and Saini S. BRN4 is a novel driver of neuroendocrine differentiation in castration-resistant prostate cancer and is selectively released in extracellular vesicles with BRN2. Clin Cancer Res 2019; 25: 6532-6545.
[26] Bishop JL, Thaper D, Vahid S, Davies A, Ketola K, Kuruma H, Jama R, Nip KM, Angeles A, Johnson F, Wyatt AW, Fazli L, Gleave ME, Lin D, Rubin MA, Collins CC, Wang Y, Beltran H and Zoubeidi A. The master neural transcription factor BRN2 is an androgen receptor-suppressed driver of neuroendocrine differentiation in prostate cancer. Cancer Discov 2017; 7: 54-71.
[27] Yasumizu Y, Rajabi H, Jin C, Hata T, Pitroda S, Long MD, Hagiwara M, Li W, Hu Q, Liu S, Yamashita N, Fushimi A, Kui L, Samur M, Yamamoto M, Zhang Y, Zhang N, Hong D, Maeda T, Kosaka T, Wong KK, Oya M and Kufe D. MUC1-C regulates lineage plasticity driving progression to neuroendocrine prostate cancer. Nat Commun 2020; 11: 338.
[28] Davies AH, Beltran H and Zoubeidi A. Cellular plasticity and the neuroendocrine phenotype in prostate cancer. Nat Rev Urol 2018; 15: 271-286.
[29] Nijhout HF. Development and evolution of adaptive polyphenisms. Evol Dev 2003; 5: 9-18.
[30] Beltran H, Rickman DS, Park K, Chae SS, Sboner A, MacDonald TY, Wang Y, Sheikh KL, Terry S, Tagawa ST, Dhir R, Nelson JB, de la Taille A, Allory Y, Gerstein MB, Perner S, Pienta KJ, Chinnaiyan AM, Wang Y, Collins CC, Gleave ME, Demichelis F, Nanus DM and Rubin MA. Molecular characterization of neuroendocrine prostate cancer and identification of new drug targets. Cancer Discov 2011; 1: 487-495.
[31] Quintanal-Villalonga A, Chan JM, Yu HA, Pe'er D, Sawyers CL, Sen T and Rudin CM. Lineage plasticity in cancer: a shared pathway of therapeutic resistance. Nat Rev Clin Oncol 2020; 17: 360-371.
[32] Boumahdi S and de Sauvage FJ. The great escape: tumour cell plasticity in resistance to targeted therapy. Nat Rev Drug Discov 2020; 19: 39-56.
[33] Chang YT, Lin TP, Tang JT, Campbell M, Luo YL, Lu SY, Yang CP, Cheng TY, Chang CH, Liu TT, Lin CH, Kung HJ, Pan CC and Chang PC. HOTAIR is a REST-regulated lncRNA that promotes neuroendocrine differentiation in castration resistant prostate cancer. Cancer Lett 2018; 433: 43-52.
[34] Flores-Morales A, Bergmann TB, Lavallee C, Batth TS, Lin D, Lerdrup M, Friis S, Bartels A, Kristensen G, Krzyzanowska A, Xue H, Fazli L, Hansen KH, Roder MA, Brasso K, Moreira JM, Bjartell A, Wang Y, Olsen JV, Collins CC and Iglesias-Gato D. Proteogenomic characterization of patient-derived xenografts highlights the role of REST in neuroendocrine differentiation of castration-resistant prostate cancer. Clin Cancer Res 2019; 25: 595-608.
[35] Liang H, Studach L, Hullinger RL, Xie J and Andrisani OM. Down-regulation of RE-1 silencing transcription factor (REST) in advanced prostate cancer by hypoxia-induced miR-106b~25. Exp Cell Res 2014; 320: 188-199.

[36] Lin TP, Chang YT, Lee SY, Campbell M, Wang TC, Shen SH, Chung HJ, Chang YH, Chiu AW, Pan CC, Lin CH, Chu CY, Kung HJ, Cheng CY and Chang PC. REST reduction is essential for hypoxia-induced neuroendocrine differentiation of prostate cancer cells by activating autophagy signaling. Oncotarget 2016; 7: 26137-26151.

[37] Svensson C, Ceder J, Iglesias-Gato D, Chuan YC, Pang ST, Bjartell A, Martinez RM, Bott L, Helczynski L, Ulmert D, Wang Y, Niu Y, Collins C and Flores-Morales A. REST mediates androgen receptor actions on gene repression and predicts early recurrence of prostate cancer. Nucleic Acids Res 2014; 42: 999-1015.

[38] Zhang X, Coleman IM, Brown LG, True LD, Kollath L, Lucas JM, Lam HM, Dumpit R, Corey E, Chery L, Lakely B, Higano CS, Montgomery B, Roudier M, Lange PH, Nelson PS, Vessella RL and Morrissey C. SRRM4 Expression and the loss of REST activity may promote the emergence of the neuroendocrine phenotype in castration-resistant prostate cancer. Clin Cancer Res 2015; 21: 4698-4708.

[39] Zhu Y, Liu C, Cui Y, Nadiminty N, Lou W and Gao AC. Interleukin-6 induces neuroendocrine differentiation (NED) through suppression of RE-1 silencing transcription factor (REST). Prostate 2014; 74: 1086-1094.

[40] Chang PC, Wang TY, Chang YT, Chu CY, Lee CL, Hsu HW, Zhou TA, Wu Z, Kim RH, Desai SJ, Liu S and Kung HJ. Autophagy pathway is required for IL-6 induced neuroendocrine differentiation and chemoresistance of prostate cancer LNCaP cells. PLoS One 2014; 9: e88556.

[41] Ooi L and Wood IC. Chromatin crosstalk in development and disease: lessons from REST. Nat Rev Genet 2007; 8: 544-554.

[42] Lietz M, Hohl M and Thiel G. RE-1 silencing transcription factor (REST) regulates human synaptophysin gene transcription through an intronic sequence-specific DNA-binding site. Eur J Biochem 2003; 270: 2-9.

[43] Ge R, Wang Z, Montironi R, Jiang Z, Cheng M, Santoni M, Huang K, Massari F, Lu X, Cimadamore A, Lopez-Beltran A and Cheng L. Epigenetic modulations and lineage plasticity in advanced prostate cancer. Ann Oncol 2020; 31: 470-479.

[44] Davies A, Zoubeidi A and Selth LA. The epigenetic and transcriptional landscape of neuroendocrine prostate cancer. Endocr Relat Cancer 2020; 27: R35-R50.

[45] Hanly DJ, Esteller M and Berdasco M. Interplay between long non-coding RNAs and epigenetic machinery: emerging targets in cancer? Philos Trans R Soc Lond B Biol Sci 2018; 373: 20170074.

[46] Gupta RA, Shah N, Wang KC, Kim J, Horlings HM, Wong DJ, Tsai MC, Hung T, Argani P, Rinn JL, Wang Y, Brzoska P, Kong B, Li R, West RB, van de Vijver MJ, Sukumar S and Chang HY. Long non-coding RNA HOTAIR reprograms chromatin state to promote cancer metastasis. Nature 2010; 464: 1071-1076.

[47] Khalil AM, Guttman M, Huarte M, Garber M, Raj A, Rivea Morales D, Thomas K, Presser A, Bernstein BE, van Oudenaarden A, Regev A, Lander ES and Rinn JL. Many human large intergenic noncoding RNAs associate with chromatin-modifying complexes and affect gene expression. Proc Natl Acad Sci U S A 2009; 106: 11667-11672.

[48] Tsai MC, Manor O, Wan Y, Mosammaparast N, Wang JK, Lan F, Shi Y, Segal E and Chang HY. Long noncoding RNA as modular scaffold of histone modification complexes. Science 2010; 329: 689-693.

[49] Wang KC and Chang HY. Molecular mechanisms of long noncoding RNAs. Mol Cell 2011; 43: 904-914.

[50] Fatica A and Bozzoni I. Long non-coding RNAs: new players in cell differentiation and development. Nat Rev Genet 2014; 15: 7-21.

[51] Flynn RA and Chang HY. Long noncoding RNAs in cell-fate programming and reprogramming. Cell Stem Cell 2014; 14: 752-761.

[52] Schmitt AM and Chang HY. Long noncoding RNAs in cancer pathways. Cancer Cell 2016; 29: 452-463.

[53] Liu T, Han C, Fang P, Zhu H, Wang S, Ma Z, Zhang Q, Xia W, Wang J, Xu L and Yin R. Long non-coding RNAs in lung cancer: implications for lineage plasticity-mediated TKI resistance. Cell Mol Life Sci 2021; 78: 1983-2000.

[54] Crea F. Neuroendocrine prostate cancer: long noncoding RNAs to treat an incurable cancer - an interview with Dr Francesco Crea. Epigenomics 2019; 11: 1461-1462.

[55] Ramnarine VR, Alshalalfa M, Mo F, Nabavi N, Erho N, Takhar M, Shukin R, Brahmbhatt S, Gawronski A, Kobelev M, Nouri M, Lin D, Tsai H, Lotan TL, Karnes RJ, Rubin MA, Zoubeidi A, Gleave ME, Sahinalp C, Wyatt AW, Volik SV, Beltran H, Davicioni E, Wang Y and Collins CC. The long noncoding RNA landscape of neuroendocrine prostate cancer and its clinical implications. Gigascience 2018; 7: giy050.

[56] Crea F, Venalainen E, Ci X, Cheng H, Pikor L, Parolia A, Xue H, Nur Saidy NR, Lin D, Lam W, Collins C and Wang Y. The role of epigenetics and long noncoding RNA MIAT in neuroendocrine prostate cancer. Epigenomics 2016; 8: 721-731.

[57] Luo J, Wang K, Yeh S, Sun Y, Liang L, Xiao Y, Xu W, Niu Y, Cheng L, Maity SN, Jiang R and Chang C. LncRNA-p21 alters the antiandrogen enzalutamide-induced prostate cancer neuroendocrine differentiation via modulating the EZH2/STAT3 signaling. Nat Commun 2019; 10: 2571.

[58] Chang YT, Lin TP, Campbell M, Pan CC, Lee SH, Lee HC, Yang MH, Kung HJ and Chang PC. REST is a crucial regulator for acquiring EMT-like and stemness phenotypes in hormone-refractory prostate cancer. Sci Rep 2017; 7: 42795.

[59] Xie C, Yuan J, Li H, Li M, Zhao G, Bu D, Zhu W, Wu W, Chen R and Zhao Y. NONCODEv4: exploring the world of long non-coding RNA genes. Nucleic Acids Res 2014; 42: D98-103.

[60] Leiblich A, Cross SS, Catto JW, Pesce G, Hamdy FC and Rehman I. Human prostate cancer cells express neuroendocrine cell markers PGP 9.5 and chromogranin A. Prostate 2007; 67: 1761-1769.

[61] Delk NA and Farach-Carson MC. Interleukin-6: a bone marrow stromal cell paracrine signal that induces neuroendocrine differentiation and modulates autophagy in bone metastatic PCa cells. Autophagy 2012; 8: 650-663.

[62] Sweeney CJ, Chen YH, Carducci M, Liu G, Jarrard DF, Eisenberger M, Wong YN, Hahn N, Kohli M, Cooney MM, Dreicer R, Vogelzang NJ, Picus J, Shevrin D, Hussain M, Garcia JA and DiPaola RS. Chemohormonal therapy in metastatic hormone-sensitive prostate cancer. N Engl J Med 2015; 373: 737-746.

[63] Ballas N and Mandel G. The many faces of REST oversee epigenetic programming of neuronal genes. Curr Opin Neurobiol 2005; 15: 500-506.

[64] Zuccato C, Tartari M, Crotti A, Goffredo D, Valenza M, Conti L, Cataudella T, Leavitt BR, Hayden MR, Timmusk T, Rigamonti D and Cattaneo E. Huntingtin interacts with REST/NRSF to modulate the transcription of NRSE-controlled neuronal genes. Nat Genet 2003; 35: 76-83.

[65] Westbrook TF, Hu G, Ang XL, Mulligan P, Pavlova NN, Liang A, Leng Y, Maehr R, Shi Y, Harper JW and Elledge SJ. SCFbeta-TRCP controls oncogenic transformation and neural differentiation through REST degradation. Nature 2008; 452: 370-374.

[66] Mulligan P, Westbrook TF, Ottinger M, Pavlova N, Chang B, Macia E, Shi YJ, Barretina J, Liu J, Howley PM, Elledge SJ and Shi Y. CDYL bridges REST and histone methyltransferases for gene repression and suppression of cellular transformation. Mol Cell 2008; 32: 718-726.

[67] Lapuk AV, Wu C, Wyatt AW, McPherson A, McConeghy BJ, Brahmbhatt S, Mo F, Zoubeidi A, Anderson S, Bell RH, Haegert A, Shukin R, Wang Y, Fazli L, Hurtado-Coll A, Jones EC, Hach F, Hormozdiari F, Hajirasouliha I, Boutros PC, Bristow RG, Zhao Y, Marra MA, Fanjul A, Maher CA, Chinnaiyan AM, Rubin MA, Beltran H, Sahinalp SC, Gleave ME, Volik SV and Collins CC. From sequence to molecular pathology, and a mechanism driving the neuroendocrine phenotype in prostate cancer. J Pathol 2012; 227: 286-297.

[68] Lin YC, Chang YT, Campbell M, Lin TP, Pan CC, Lee HC, Shih JC and Chang PC. MAOA-a novel decision maker of apoptosis and autophagy in hormone refractory neuroendocrine prostate cancer cells. Sci Rep 2017; 7: 46338.

[69] Derrien T, Johnson R, Bussotti G, Tanzer A, Djebali S, Tilgner H, Guernec G, Martin D, Merkel A, Knowles DG, Lagarde J, Veeravalli L, Ruan X, Ruan Y, Lassmann T, Carninci P, Brown JB, Lipovich L, Gonzalez JM, Thomas M, Davis CA, Shiekhattar R, Gingeras TR, Hubbard TJ, Notredame C, Harrow J and Guigo R. The GENCODE v7 catalog of human long noncoding RNAs: analysis of their gene structure, evolution, and expression. Genome Res 2012; 22: 1775-1789.

[70] de Kok JB, Verhaegh GW, Roelofs RW, Hessels D, Kiemeney LA, Aalders TW, Swinkels DW and Schalken JA. DD3(PCA3), a very sensitive and specific marker to detect prostate tumors. Cancer Res 2002; 62: 2695-2698.

[71] Lemos AEG, Matos ADR, Ferreira LB and Gimba ERP. The long non-coding RNA PCA3: an update of its functions and clinical applications as a biomarker in prostate cancer. Oncotarget 2019; 10: 6589-6603.

[72] Gana S, Veggiotti P, Sciacca G, Fedeli C, Bersano A, Micieli G, Maghnie M, Ciccone R, Rossi E, Plunkett K, Bi W, Sutton VR and Zuffardi O. 19q13.11 cryptic deletion: description of two new cases and indication for a role of WTIP haploinsufficiency in hypospadias. Eur J Hum Genet 2012; 20: 852-856.

[73] Chowdhury S, Bandholz AM, Parkash S, Dyack S, Rideout AL, Leppig KA, Thiese H, Wheeler PG, Tsang M, Ballif BC, Shaffer LG, Torchia BS, Ellison JW and Rosenfeld JA. Phenotypic and molecular characterization of 19q12q13.1 deletions: a report of five patients. Am J Med Genet A 2014; 164A: 62-69.

[74] Yamamura S, Imai-Sumida M, Tanaka Y and Dahiya R. Interaction and cross-talk between non-coding RNAs. Cell Mol Life Sci 2018; 75: 467-484.

[75] You L, Wang Z, Li H, Shou J, Jing Z, Xie J, Sui X, Pan H and Han W. The role of STAT3 in autophagy. Autophagy 2015; 11: 729-739.

[76] Chen S, Mari M, Parashar S, Liu D, Cui Y, Reggiori F, Novick PJ and Ferro-Novick S. Vps13 is required for the packaging of the ER into autophagosomes during ER-phagy. Proc Natl Acad Sci U S A 2020; 117: 18530-18539.

Table S1. Primer sequences for RT-qPCR used in this study

Gene	Forward primer (5'-3')	Reverse primer (5'-3')
ATG2B	GCTCACAAGTTACTTCAGCTC	ATCAACATCCAACTTAGCTCC
ATM	CAATCATCACCAAGTTCGCA	CAGCACTATGGGACATTTCTC
BIRC2	ATCTAGTGTTCCAGTTCAGCC	AACTCACACCTTGGAAACCAC
BIRC6	ATCATGTTCAGTTGGAGTCAC	CTATGAAGCACAAGGCACC
CHUK	TGTTACCACCTGATGAAAGTC	CTATCACAGCCTCTAACTCCA
COPZ1	GGACTGACAGTGAAATTGCC	TTCATCCACAGCCAAGAACAG
GNAI3	TCCCAGTCTAACTACATTCCA	GCATTCGGTTCATCTCCTC
HIF1A	AGTTCACCTGAGCCTAATAGTCC	TCCAAGTCTAAATCTGTGTCCTG
MCL1	CCTTCCAAGGCATGCTTCG	GGAAGAACTCCACAAACCCA
MFN1	GTTAGTAGACAGTCCAGGCA	GGCATCCCAACGATTATTGAG
PTEN	CGGAACTTGCAATCCTCAG	ACGCTCTATACTGCAAATGCT
RB1CC1	TGACGTAACTGTATCAGAGGG	ATTTGTATCCGTCCCAGCAC
ROCK1	TTACTGACAGGGAAGTGAGG	ACTTAAATCGGGTACAACTGG
SCOC	TTAAGAATGCAACACTCAGGTC	GAGGAATGGTCTATGTCATCTG
STAM2	TTCCAATGCAGACATATCCAG	TGACATATCCACAGACATCCC
TBK1	ACATAAGCTTCCTTCGTCCA	CATTCCACCCACCACATCTC
VPS13A	AGTTCAAACCTGATGTGCCT	TTCCAACTCCTCCAAAGACAC
XPO1	CGCAGATACGGGCTTACAG	ACCAGCAGTATGTGAAGTGTC